EUKARYOTIC CELL, Aug. 2004, p. 992–1003 Vol. 3, No. 4
1535-9778/04/$08.00+0 DOI: 10.1128/EC.3.4.992–1003.2004

Dynamics of *Toxoplasma gondii* Differentiation†

Florence Dzierszinski, Manami Nishi, Lillian Ouko, and David S. Roos*

Department of Biology, University of Pennsylvania, Philadelphia, Pennsylvania 19104-6018

Received 13 April 2004/Accepted 4 June 2004

Parasite differentiation is commonly associated with transitions between complex life cycle stages and with long-term persistence in the host, and it is therefore critical for pathogenesis. In the protozoan parasite *Toxoplasma gondii*, interconversion between rapidly growing tachyzoites and latent encysted bradyzoites is accompanied by numerous morphological and metabolic adaptations. In order to explore early cell biological events associated with this differentiation process, we have exploited fluorescent reporter proteins targeted to various subcellular locations. Combining these markers with efficient in vitro differentiation and time-lapse video microscopy provides a dynamic view of bradyzoite development in living cultures, demonstrating subcellular reorganization, maintenance of the mitochondrion, and missegregation of the apicoplast. Bradyzoites divide asynchronously, using both endodyogeny and endopolygeny, and are highly motile both within and between host cells. Cysts are able to proliferate without passing through an intermediate tachyzoite stage, via both the migration of free bradyzoites and the fission of bradyzoite cysts, suggesting a mechanism for dissemination during chronic infection.

Differentiation in unicellular organisms is a temporal phenomenon, often associated with altered environmental conditions. For many protozoan parasites, differentiation is an obligatory process, with distinct life cycle stages required for transmission between host and vector organisms. *Toxoplasma gondii* is a ubiquitous member of the phylum *Apicomplexa*, which also includes thousands of other parasite species (29), many of them serious human and veterinary pathogens with complex life cycles (such as the bloodstream, liver, and various mosquito stages of *Plasmodium* parasites that cause malaria).

The sexual cycle of *T. gondii* occurs only in feline intestinal epithelium, yielding sporozoites within environmentally stable oocysts in the feces (21). Two asexual forms (acutely lytic tachyzoites and latent bradyzoite tissue cysts) may be found in a wide range of intermediate hosts, including most tissues of any homeothermic vertebrate. Bradyzoites appear to be the direct precursor to sexual stages, producing oocysts in cats with prepatent periods as short as 3 days (10). Infection is acquired through ingestion of either meat from infected animals containing tissue cysts (bradyzoites) or soil contaminated with feline fecal matter containing oocysts (sporozoites). Passage through the gut releases sporozoites or bradyzoites, which invade the intestinal epithelium and rapidly differentiate into tachyzoites. Acute infection is usually controlled by the host immune response, but tachyzoite transmission to the developing fetus can be devastating, making *T. gondii* a leading cause of congenital neurological birth defects in humans. In healthy adults, a small percentage of tachyzoites differentiate, forming slowly replicating bradyzoites in the brain, muscles, and other organs, where they may remain viable as a chronic infection for the life of the host. *T. gondii* infection therefore poses a threat to immunocompromised patients (31).

* Corresponding author. Mailing address: Department of Biology, University of Pennsylvania, Philadelphia PA 19104-6018. Phone: (215) 898-2118. Fax: (215) 746-6697. E-mail: droos@sas.upenn.edu.

† Supplemental material for this article may be found at http://ec.asm.org.

In vivo, bradyzoites are thought to be metabolically quiescent, replicating very slowly within tissue cysts, but they remain viable and therefore ensure persistence of the infection. Morphological studies on fixed specimens (reviewed in reference 11) have shown that encysted bradyzoites isolated from the brain differ from tachyzoites in various respects, including the following: (i) modification of the parasitophorous vacuole (PV) membrane by addition of chitin, glycoproteins, and possibly glycolipids to form a cyst wall (5, 61); (ii) accumulation of amylopectin granules, reflecting substantial glucose storage; and (iii) subcellular reorganization (relocation of the nucleus in a more posterior location and redistribution of the secretory organelles important for host cell invasion, establishment, modification, and maintenance of the PV). Precisely how and when these modifications occur remain unclear. New tissue cyst formation in the brain has been reported as older cysts break down during chronic infection, but the factors governing this process are also unknown (11, 17).

Various bradyzoite-specific markers are available (reviewed in reference 58), and several systems have been developed to study *T. gondii* differentiation in vitro (4, 46, 52, 57, 59). Unfortunately, the heterogeneity of in vitro differentiation complicates analysis of bradyzoite populations (45). Moreover, differentiation is asynchronous and bradyzoite cultures are typically overgrown by rapidly dividing tachyzoites, but more extreme differentiation conditions may be toxic and therefore detrimental to long-term culture maintenance. We have optimized culture conditions to maximize bradyzoite differentiation, permitting this process to be studied for up to 2 weeks in vitro. We have also exploited a variety of transgenic parasites in which fluorescent protein reporters have been engineered to label distinct subcellular organelles (23, 25, 48–50), helping to validate the in vitro differentiation system and permitting the differentiation of individual cells to be followed in real time, using time-lapse video microscopy. These studies yield new insights into the biology of immature bradyzoites, host cell invasion, and parasite dissemination.

MATERIALS AND METHODS

Cell and parasite cultivation. ΔHXGPRT knockout mutants derived from the avirulent Prugniaud strain of *T. gondii* parasites were kindly provided by D. Soldati (Imperial College, London, United Kingdom); yellow fluorescent protein (YFP)- or green fluorescent protein (GFP)-expressing stable transgenics were engineered as described below. Tachyzoites were maintained by serial passage in human foreskin fibroblast cell monolayers, in Dulbecco's modified Eagle's medium (Gibco) containing 10% fetal bovine serum as previously described (42). For microscopy, monolayers were grown on 22-mm glass coverslips or (for time-lapse video microscopy) gridded coverslip-bottom 35-mm dishes (MatTek Corporation, Ashland, Mass.). Host cell viability was assessed by exclusion of trypan blue (0.2% in phosphate-buffered saline [PBS]).

Unless otherwise indicated, in vitro bradyzoite differentiation was induced in minimal essential medium (Gibco) containing Earle's salts (5.3 mM KCl) without $NaHCO_3$, buffered to pH 7.2 with 25mM HEPES, and maintained at 37°C in 0.03% (ambient) CO_2, as previously described (4). To test the effects of environmental conditions on developing bradyzoites, [KCl] was increased to 45 or 90 mM and pH was changed to 6.2 or 8.2. For bradyzoite purification, infected cells were induced for up to 28 days, harvested with 0.25% trypsin in 1 mM EDTA to minimize possible rupture of the cysts, and washed in PBS.

Mature bradyzoite cysts were induced in CBA mice by intraperitoneal injection of 20 strain ME49 cysts or 10^5 *pbag1*-YFP tachyzoites and maintained for 1 to 8 weeks before harvesting the mouse brains, homogenization, and purification by isopycnic centrifugation on a Percoll gradient.

Molecular methods. Clonal transgenic lines were engineered to constitutively express YFP or GFP in various subcellular locations and red fluorescent protein (RFP) in the cytosol under the control of the bradyzoite-specific promoter *BAG1* (3). YFP- and GFP-targeting vectors were based on pBluescript KS(+) (Stratagene) and contained the following elements: (i) the *T. gondii TUB1* promoter (39), terminating at a BglII site upstream of the initiation codon; (ii) coding sequences as described below, terminating in an AvrII site cloned in frame with a fluorescent reporter; (iii) a 3′ untranslated region from the *T. gondii* DHFR-TS gene, terminating in a NotI site (41); and (iv) a chloramphenicol acetyltransferase (CAT) selectable marker expressed under the control of 5′ and 3′ untranslated regions derived from the *T. gondii SAG1* gene (27).

Plasmid *ptub*ROPI-YFP/*sag*CAT was constructed by replacing the GFP-3′*dhfr* AvrII/NotI restriction fragment in *ptub*ROP1-GFP/*sag*CAT (48) with YFP-3′*dhfr*. Plasmids *ptub*YFP-αTUB/*sag*CAT, *ptub*MIC3-GFP, and *ptub*IMC1-YFP/*sag*CAT have been previously described (25, 49, 50). Plasmid *ptub*FNR-YFP/*sag*CAT (kindly provided by F. Seeber, Philipps-Universität, Marburg, Germany) contains the first 150 amino acids (signal and transit peptides) of the *T. gondii* ferredoxin-$NADP^+$ reductase (FNR) (55). This plasmid was used as the basis for *ptub*GRA8-YFP/*sag*CAT (M. J. Crawford, unpublished data), constructed by replacing the FNR leader peptide with amino acids 1 to 24 of the GRA8 signal peptide, amplified using primers 5′BglII-CATAGATCT**ATG**GCTTTACCATT GCGTGTTTCGG-3′ (ATG indicates the translation initiation codon) and 5′NheI-CTAGCTAGCGCGAGCTACACCAAAGACAGC-3′ (restriction sites are underlined). Plasmid *ptub*P30-YFP-HDEL was generated by first replacing the FNR leader with the P30 signal peptide (primers 5′-GGAAGATCT**ATG**T CGGTTTCGCTGCAC-3′ and 5′-GCATCCTAGGCGCGACACAAGCTGCG AT-3′) to generate *ptub*P30-YFP/*sag*CAT. The HDEL peptide was then introduced at the C terminus of YFP (primers 5′-GGAAGATCT**ATG**TCGGTTTC GCTGCAC-3′ and 5′-GCATCTTAAGCTACAACTCGTCGTGCTTGTACA GCTCGTCC-3′), and P30-YFP-HDEL was cloned in *ptub*[BglII]GFP[AflII] 3′*dhfr*[NotI]/*sag*CAT as a BglII/AflII fragment. Plasmid *ptub*HSP60-YFP/*sag*CAT was made by replacing the FNR leader peptide with the heat shock protein 60 (HSP60) signal peptide (amino acids 1 to 55) as a BglII/AvrII fragment after PCR amplification from *T. gondii* cDNA (primers 5′-ATGCAGAT CTAAA**ATG**CTTGCCCGCGCTTCAG-3′ and 5′-CAGTCCTAGGGCCGAG AGTGACTCCGAC-3′). Plasmid *pbag1*P30GFP/*sag*CAT (W. Bohne and D. S. Roos, unpublished data) was used to generate *pbag1*RFP/*sag*CAT by subcloning an RFP-3′*dhfr* fragment in place of the P30GFP-3′*dhfr* fragment via BglII/NotI restriction digests. The RFP-3′*dhfr* fragment was produced by BglII/NotI digestion of plasmid *ptub*RFP/*sag*CAT. RFP was originally subcloned in the upstream BglII and downstream AflII sites of *ptub*[BglII]GFP[AflII]3′*dhfr*[NotI]/*sag*CAT after PCR amplification from *p*DsRed1-1 (Clontech) (primers 5′-AGATCTAA A**ATG**GCGCGCTCCTCCAAGAACGTC-3′ and 5′-CTTAAGTTACAGGAA CAGGTGGTGGCGGCC-3′). To improve the level of expression of RFP in *T. gondii*, the second codon of DsRed was modified to encode an alanine residue (33).

Transfections were performed by electroporation as previously described (42), using 2×10^7 tachyzoites and 70 μg of each plasmid (YFP construct and *pbag1*RFP) as NotI-linearized DNA, in a 2-mm-gap cuvette (BTX; 1.5-kEV pulse, 24 Ω). Stable transgenics were selected in the presence of 20 μM chloramphenicol for all plasmids but *ptub*MIC3-GFP. The parasite line stably expressing MIC3-GFP was obtained by cotransfection with 10 μg of *p*DHFR-TSc3 (9) and selection in 1 μM pyrimethamine. Parasite clones were isolated by limiting dilution after drug selections. All fluorescent transgenic clones except for Prugniaud ROP1-YFP and MIC3-GFP were also engineered to stably express *pbag*1RFP.

Microscopy and imaging. For fluorescence labeling experiments (after the conclusion of time-lapse video microscopy), culture dishes were fixed in 4% (wt/vol) paraformaldehyde in PBS and permeabilized in 0.2% (vol/vol) Triton X-100. The following antibody reagents were used: monoclonal anti-MIC3 and anti-ROP2/3/4 antibodies (from J. F. Dubremetz, University Montpellier, Montpellier, France), monoclonal anti-IMC1 antibody (from G. Ward, University of Vermont), rabbit anti-ACP antibody (from G. I. McFadden, University of Melbourne, Melbourne, Australia), mouse monoclonal or rabbit anti-GFP antibodies (Clontech). All antibodies were diluted 1:1,000 in 10% (vol/vol) fetal bovine serum–0.1% Triton X-100 (in PBS) and detected using AlexaFluor 488-conjugated goat anti-mouse or anti-rabbit immunoglobulin G (IgG) antibodies, AlexaFluor 594-conjugated goat anti-mouse or anti-rabbit IgG antibodies, or AlexaFluor 350-conjugated goat anti-mouse IgG antibody (Molecular Probes). Nuclear and apicoplast DNA were visualized by staining with 2.8 μM 4′,6′-diamidino-2-phenylindole (DAPI; Molecular Probes), and the bradyzoite cyst wall was visualized by staining with tetramethyl rhodamine isothiocyanate-conjugated *Dolichos biflorus* lectin (Sigma) (5).

YFP, GFP, RFP, DAPI, and secondary fluorescent reagents were detected using a Zeiss Axiovert 35 microscope equipped with a 100-W Hg vapor lamp, appropriate barrier-emission filters, and an interline transfer chip charge-coupled device camera (Hamamatsu). For time-lapse video microscopy, imaging was performed at 37°C using a heated microscope stage and lens objective heater (Bioptechs). Images were captured, colored, and contrast-adjusted using Openlab software (Improvision). Images shown are representative of the observations made on at least 50 vacuoles in several independent experiments followed by time-lapse video under bradyzoite differentiation conditions. Observations were also performed on a Zeiss LSM510 confocal microscope using an Ar/Kr laser (488-nm line) and an Olympus IX70 inverted microscope equipped with a 100-W Hg vapor lamp with appropriate barrier-emission filters (DeltaVision). When using the Olympus IX70 inverted microscope, images were captured using a Photometrics CoolSNAP Hi Res charge-coupled device camera and DeltaVision softWorx software (Applied Precision).

Videos related to this work are available in the supplemental material.

RESULTS

Immature bradyzoites and quasi-mature cysts in vitro. GFP and YFP were expressed under control of the constitutive *TUB1* promoter in order to investigate early stages of parasite differentiation in vitro. Because differentiation is asynchronous, we used time-lapse video microscopy to follow individual PVs over the course of several days, providing a dynamic view of this process. Most reports on *T. gondii* differentiation in vitro have not permitted observation for more than 3 to 4 days after induction because host cells are killed by either the induction conditions or tachyzoite outgrowth, but CO_2 depletion (4) was highly effective at inducing differentiation in the cyst-forming Prugniaud strain. Trypan blue staining demonstrated that infected host cells remained viable for >8 days in the dishes used for time-lapse microscopy, for 2 weeks on coverslips, and for up to 1 month in cell culture flasks.

Figure 1A shows that parasites induced for 10 days in vitro are surrounded by a highly refractile cyst wall and express the bradyzoite-specific *BAG1* promoter (here used to drive expression of RFP). Cyst rupture was occasionally observed in vitro, revealing zoites that were slimmer than tachyzoites and capable of dividing by endodyogeny (Fig. 1B). Transgenic parasites expressing YFP also produced mature tissue cysts in the brains

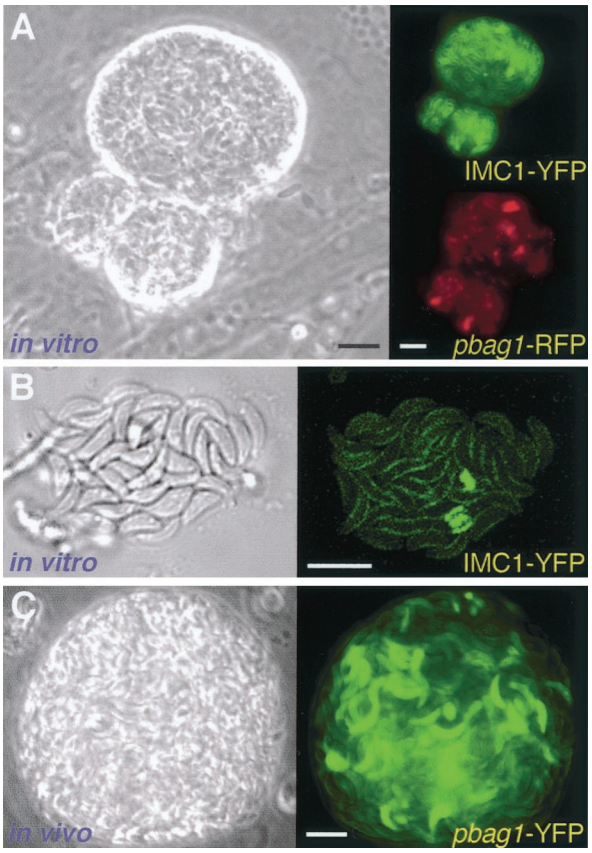

FIG. 1. Fluorescent bradyzoites in vitro and in vivo. (A) Phase-contrast image showing the refractile wall surrounding a parasite cyst obtained after 10 days of bradyzoite induction in vitro. These transgenic parasites express *ptub*IMC1-YFP/*pbag1*RFP, demonstrating expression from the bradyzoite-specific promoter *bag1* (red). YFP imaging of the inner membrane complex (green) indicates that few parasites are replicating (IMC1-YFP labeling is more intense in replicating parasites [25]). (B) Confocal differential interference contrast microscopy and fluorescence imaging of a recently ruptured 15-day-old in vitro cyst reveals slim bradyzoites. In contrast to the rapid synchronous division characteristic of tachyzoites (19), replication within developing bradyzoite cysts is asynchronous, with very few parasites engaged in division. (C) Tissue cysts isolated from the brain of a mouse infected with *pbag1*-YFP transgenic parasites exhibit strong expression of the fluorescent reporter. Note similarities between the quasi-mature cysts obtained in vitro and in vivo. The relatively nonrefractile nature of the in vivo cyst shown is attributable to the equatorial optical section plane in this unfixed specimen. Bars, 10 μm. (See also the time-lapse videos in the supplemental material.)

of infected mice (Fig. 1C) with a morphology that was virtually indistinguishable from in vitro cysts (11).

Bradyzoite differentiation is characterized by reduced growth rates, asynchronous replication, and a combination of endodyogeny and endopolygeny. Bradyzoites are distinguished from tachyzoites by their much slower growth rate, and reduced replication rates were consistently observed during differentiation in vitro. As previously noted, the timing of differentiation differed from vacuole to vacuole. By time-lapse microscopy, reduced growth rates were observed in some vacuoles as early as the second division cycle following induction and in other vacuoles (in the same culture) as late as 4 days later (data not shown).

No differences in IMC or tubulin architecture were observed between tachyzoites and bradyzoites, but transgenic parasites expressing fluorescently labeled cytoskeletal proteins can be very useful for following cell division (25). Tachyzoites typically divide synchronously every ~7 h by endodyogeny, forming rosettes of 2, 4, 8, 16, etc., parasites within the PV (19, 44); endodyogeny has also been reported in mature bradyzoite cysts (15). Developing bradyzoites display asynchronous cycles of division as soon as parasite growth slows; as a result, vacuoles often contain unusual numbers of parasites (Fig. 2A, third panel, 22 h). Cytokinesis of immature bradyzoites often required >12 h (Fig. 2C), versus ~7 h for tachyzoites. The formation of multiple daughter parasites has been reported to occur in tachyzoites grown in vitro at a frequency of ~0.5 to 5%, depending on conditions (25). In immature bradyzoites, however, multiple daughter formation occurred at a much higher frequency (see below), and successive cycles of en-

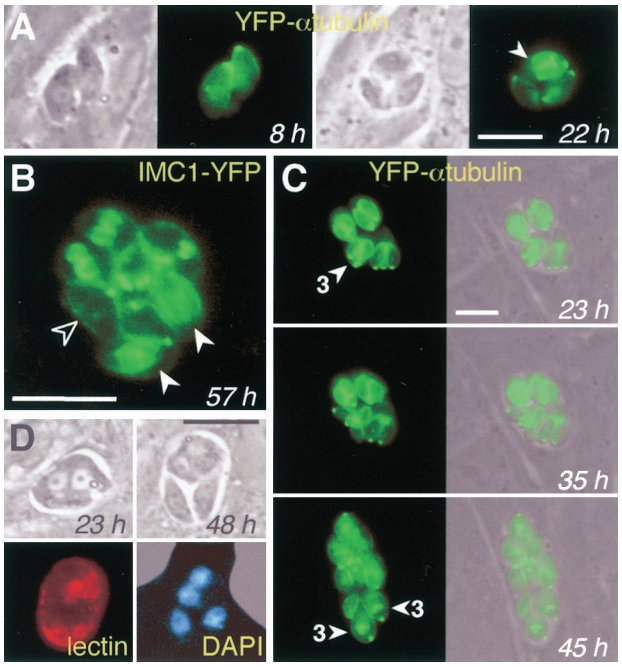

FIG. 2. Replication of developing bradyzoites by asynchronous endodyogeny and endopolygeny-schizogony. (A) As shown using time-lapse video microscopy of living parasites, asynchronous cycles of division provided an early marker of differentiation. By 22 h, one of the two parasites in the 8-h vacuole had long since divided to yield two daughters (lower two parasites), while the other parasite was just beginning to divide (arrowhead). (B) Asynchronous division visualized by the various stages of inner membrane complex assembly: one parasite has not yet begun to assemble daughter scaffolds (open arrowhead), while two have nearly completed daughter parasite assembly (filled arrowheads). Other parasites within this vacuole display intermediate stages of assembly. (C) Developing bradyzoites exhibit a high frequency of multiple daughter formation: the arrowhead indicates three daughters under assembly within a single mother parasite at 23 h. At least two parasites in the subsequent cycle went on to produce three daughters. Note that bradyzoite division proceeds slowly: daughters assembled at 23 h remained within the mother at 35 h; emergence typically takes <1 h for tachyzoites. (D) DAPI staining permits visualization of merozoites emerging from a syncytial structure. Parasite differentiation was verified by cyst wall labeling with *D. biflorus* lectin. Bars, 10 μm. Times reflect hours postinduction.

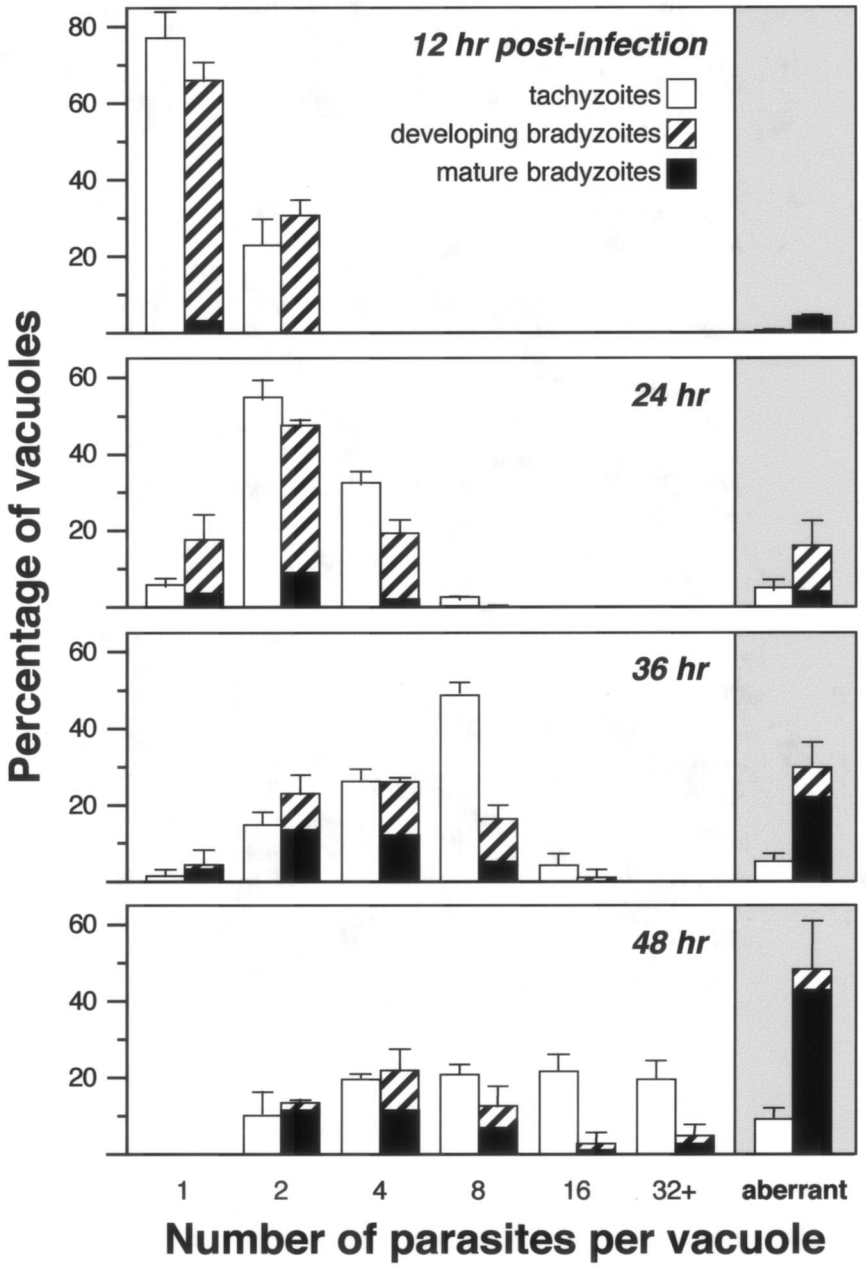

FIG. 3. Asynchronous division in developing bradyzoites. Strain Prugniaud Δ*HXGPRT* parasites were cultivated in human foreskin fibroblast cells under tachyzoite conditions (open bars) or CO_2 starvation conditions to induce bradyzoite differentiation (hatched bars). *D. biflorus* lectin staining indicated the presence of a cyst wall (black bars). The number of parasites per vacuole was determined for at least 100 vacuoles in triplicate samples at each time point. Vacuoles containing aberrant numbers of parasites (other than 2, 4, 8, etc.), indicating asynchronous division, are shown in the shaded region at right. Error bars indicate the standard deviation. Note the more rapid replication of tachyzoites versus bradyzoites and the rising frequency of asynchronous replication associated with bradyzoite differentiation (4% at 24 h, 16% at 24 h, 30% at 36 h, and 47% at 48 h).

dopolygeny or schizogony were commonly observed within a single vacuole (Fig. 2C). As many as six daughter parasites could sometimes be observed within a single mother cell. Thus, unusual numbers of parasites within a PV (i.e., other than a power of 2) are attributable to both asynchrony in cell division and, to a lesser extent, endopolygeny and schizogony. Relocation of the nucleus toward the posterior end of the parasite has been reported in morphological studies of mature cysts in vivo (11), and this relocation was also observed in vitro, beginning ~3 days after bradyzoite induction even in parasites not in the process of division (data not shown).

In order to quantify the frequency of asynchronous division during cyst formation, the number of parasites within individual PVs was examined during in vitro cultivation, as shown in Fig. 3. At 12 h postinfection, ~75% of tachyzoites contained one parasite and ~25% contained two parasites. A similar distribution was observed under bradyzoite growth conditions, and very few vacuoles had begun to differentiate, as assessed by

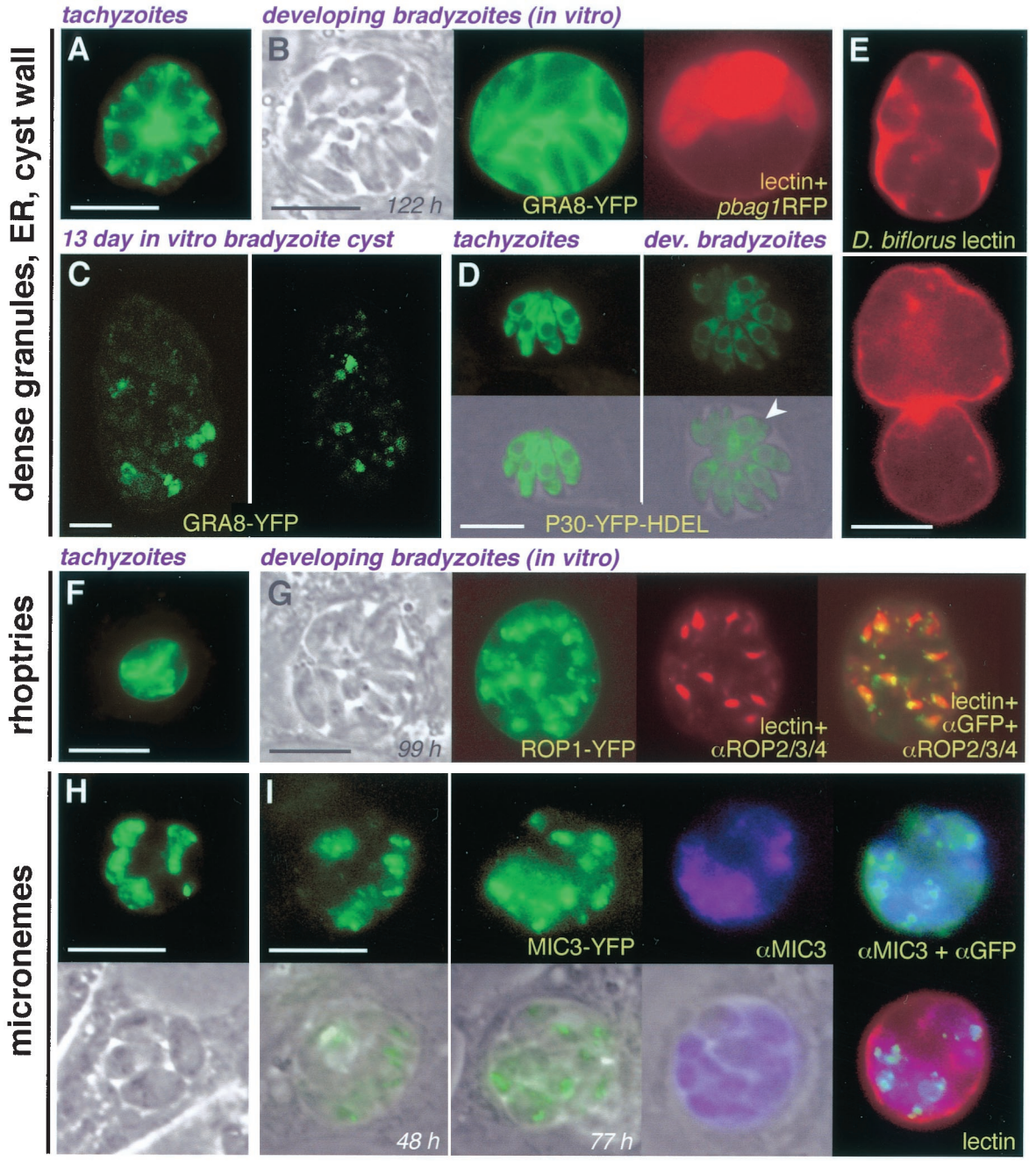

FIG. 4. Secretory compartment organization in developing bradyzoites. (A and B) Dense-granule content (GRA8-YFP) appears to be reduced early during the differentiation process, at a stage where *bag*-RFP expression is still heterogeneous: compare intracellular granules in tachyzoites (A) versus immature bradyzoites (B). (C) Later during differentiation, very little protein is visible in intracellular granules or the vacuolar space; the dense granule marker exhibited perinuclear organization characteristic of the endoplasmic reticulum (two confocal sections shown). (D) The endoplasmic reticulum marker P30-YFP-HDEL (arrowhead indicates multiple cell daughters). (E) *Dolichos* lectin staining of the PV space suggests that glycosylated cyst wall components may be secreted via dense granules early during differentiation (compare top and bottom panels). (F and G) Rhoptry organization (ROP1-YFP) was not dramatically affected during differentiation from tachyzoites (F) to bradyzoites (G). (H and I) Micronemes (MIC3-YFP) were more highly dispersed in bradyzoites (I) relative to tachyzoites (H). Bars, 10 μm. Times reflect hours postinduction.

Dolichos lectin staining. With further cultivation, the number of parasites within the PVs increased (more rapidly for tachyzoites than for bradyzoites), and the number of vacuoles containing aberrant numbers of parasites rose. Even after multiple divisions, the number of PVs in tachyzoite cultures with aberrant numbers of zoites (i.e., other than 2, 4, 8, etc.) never exceeded 10%. In contrast, coincident with bradyzoite differentiation, division in these cultures often became asynchronous: ~16% of PVs in bradyzoite cultures exhibited evidence of asynchronous replication at 24 h, increasing to ~30% at 36 h and ~47% at 48 h. The vast majority of PVs containing asynchronously dividing parasites were surrounded by a *Dolichos*-

positive cyst wall, and asynchronous replication was particularly common in vacuoles expressing the cyst wall antigen: 55% of *Dolichos*-positive vacuoles showed evidence of asynchronous replication, versus 20% of *Dolichos*-negative vacuoles cultivated under bradyzoite conditions.

In mice infected with transgenic parasites expressing both a constitutive YFP reporter and an RFP reporter under the control of the bradyzoite-specific *bag1* promoter, small numbers of undifferentiated parasite tachyzoites could be detected in the brain 1 to 2 weeks postinfection, but no bradyzoites were observed. Bradyzoite cysts were readily detected 6 to 8 weeks postinfection (cf. Fig. 1C), but the large number of zoites within these mature cysts precluded careful enumeration, making it impossible to determine frequencies of asynchronous replication.

Reorganization of secretory organelles. Reorganization of secretory organelles has previously been reported in static electron microscopic studies of mature bradyzoites isolated from mouse brain (reviewed in reference 11). As shown in Fig. 4, similar reorganization was evident when using fluorescent markers to follow the fate of these organelles during the early stages of *T. gondii* differentiation in vitro. A GRA8-YFP reporter was secreted into the PV via dense granules (Fig. 4A), but while YFP remained visible within the vacuolar space of the developing bradyzoite cysts, fewer dense granules were visible within the bradyzoites themselves (Fig. 4B). Prolonged cultivation under differentiation conditions resulted in a progressive loss of GRA8-YFP fluorescence within the PV (Fig. 4C), and most of the residual protein appeared to be retained within the endoplasmic reticulum rather than being released into the vacuolar space. Similarly, expression of an endoplasmic reticulum marker (P30-YFP-HDEL [23]) showed reduced labeling of bradyzoites versus tachyzoites within 2 days postinduction (Fig. 4D). Interestingly, cyst wall components labeled with *D. biflorus* lectin (5) appeared within the vacuolar space early in the differentiation process (Fig. 4E, top), suggesting that some of the cyst wall glycoproteins (61) may be secreted via the dense granule pathway prior to being organized into the cyst wall (Fig. 4D, bottom).

No reproducible alteration in rhoptry architecture was noted in these studies (Fig. 4F and G). Distribution of micronemes was restricted to the apical complex in tachyzoites but broadly dispersed throughout the parasite in developing bradyzoites (Fig. 4H and I), as previously described (11).

Endosymbiotic organelles: mitochondrial maintenance and apicoplast missegregation. Little is known about the metabolism or morphology of the parasite mitochondrion in *T. gondii* bradyzoites, although its ability to function during differentiation has been questioned (2, 52). An N-terminal mitochondrial targeting signal derived from *T. gondii* HSP60 was used to target YFP for time-lapse visualization of the mitochondrion during differentiation (Fig. 5). Fluorescence declined in intensity during bradyzoite induction in vitro, but mitochondrial morphology remained intact. Refractile granules of unknown composition (probably amylopectin) were detected in the cytoplasm at ~75 h postinduction (Fig. 5C), perhaps indicating changes in energy metabolism during bradyzoite differentiation.

Like most apicomplexan parasites, *T. gondii* harbors a second DNA-containing organelle, a nonphotosynthetic plastid

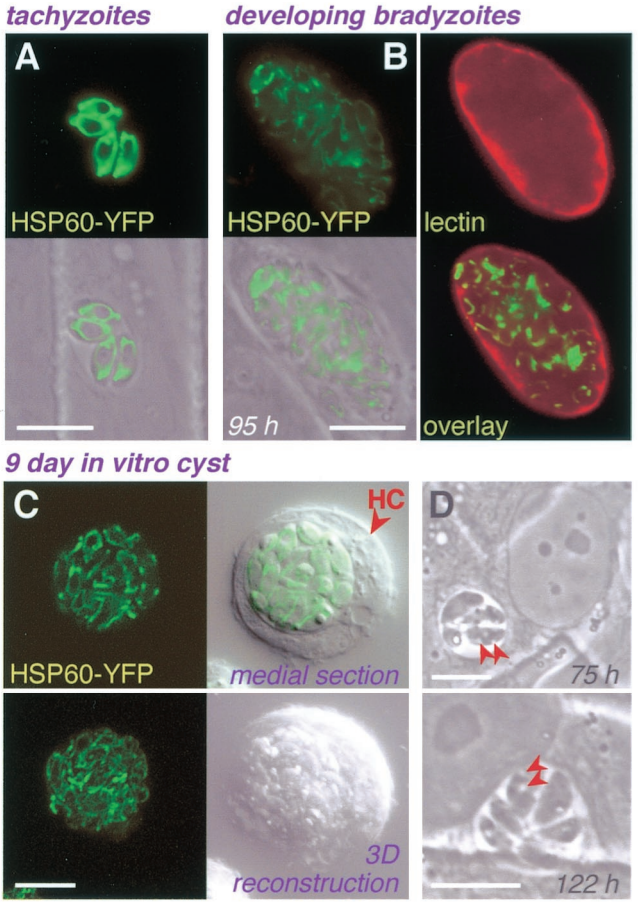

FIG. 5. Mitochondrial organization in bradyzoites. (A to C) Mitochondrial staining intensity was reduced, but organization was not substantially affected, during differentiation in vitro from tachyzoites (A), to early bradyzoite stages (B; note immature cyst wall), to 9-day-old cysts (C). (D) Cytoplasmic granules (arrows), possibly amylopectin, were detected 75 h postinduction. Except for lectin staining, panels show phase-contrast, fluorescence, or superimposed images of living parasites. HC, host cell. Bars, 10 μm.

acquired by secondary endosymbiosis (28, 43). The apicoplast is an essential organelle (20, 24) and is known to synthesize both lipids and isoprenoids (26, 56). The apicoplast is located just apical to the nucleus and is divided between daughter cells early during parasite replication (49). To examine the apicoplast in bradyzoites, we fused YFP to apicoplast-targeting signals derived from *T. gondii* FNR (55). FNR-YFP fluorescence was clearly detected in both tachyzoites and immature bradyzoites (Fig. 6A and B) and colocalized with the known apicoplast protein acyl carrier protein (ACP) (56) and DAPI-stained apicoplast DNA (data not shown).

Remarkably, ~10 to 20% of developing bradyzoite vacuoles contained individual parasites showing no FNR-YFP labeling of the apicoplast (Fig. 6C to F). Apicoplast loss was also observed in mature bradyzoite cysts generated in vivo (Fig. 6G). Lack of staining with anti-ACP and DAPI confirmed complete loss of the apicoplast in these parasites (data not shown). Anti-GFP showed that FNR-YFP was diffusely distributed in the absence of an apicoplast (Fig. 6C to E), partially colocalizing with other apical secretory organelles. Time-lapse micros-

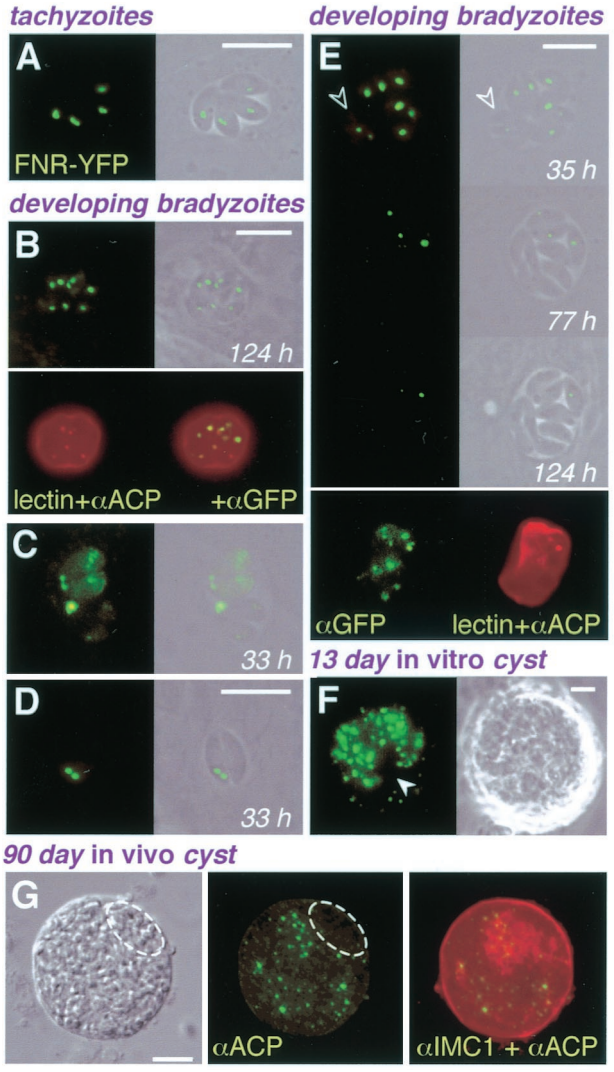

FIG. 6. Loss of the apicoplast during bradyzoite differentiation. (A to F) FNR-YFP fluorescence was detected in both tachyzoites (A) and in vitro bradyzoites (B to F) and colocalized with anti-ACP (B and E; imperfect colocalization is attributable to different focal planes). The bradyzoite cyst wall was labeled with *D. biflorus* lectin (B and E). Although the apicoplast is faithfully maintained during tachyzoite replication, this organelle was frequently lost during bradyzoite differentiation. In some cases, apicoplast loss was attributable to missegregation during division (C and D), while in other cases the organelle appeared to degenerate in the absence of replication (E). A 13-day-old in vitro cyst (F) shows parasites lacking FNR-YFP labeling (arrowhead). (G) ACP and IMC1 labeled by immunofluorescence assay in a 90-day-old tissue cyst isolated from the brain of a mouse chronically infected with wild-type ME49-B7 parasites (deconvolved images). Note the failure to detect the native apicoplast protein ACP in areas where parasites are present (as seen in the differential interference contrast image and by IMC1 labeling). Unless otherwise indicated (lectin, anti-ACP, anti-GFP, and anti-IMC1), panels show phase-contrast, fluorescence, or superimposed images of living parasites. Bars, 10 μm.Times reflect hours postinduction.

copy demonstrated several different mechanisms of apicoplast loss: (i) cases where the apicoplast failed to divide and was lost in the residual body that remained after daughter cell assembly (Fig. 6C); (ii) cases where one daughter parasite received both daughter apicoplasts (Fig. 6D); and (iii) cases where the apicoplast seemed to degenerate without parasite division (Fig. 6E; no apicoplast DNA was detected in these parasites by DAPI staining [data not shown]).

Proliferation of bradyzoite cysts. Time-lapse video microscopy permits observations of parasite behavior—as well as morphology—during bradyzoite differentiation. These studies confirmed the slow growth rates inferred from counts of intracellular parasite number. For example, the PV shown in Fig. 7A contained only two parasites after 32 h under differentiation conditions. Forty hours later, these parasites had only divided once more, to produce four parasites within the PV. Notwithstanding their slow growth, however, differentiating parasites were remarkably motile within the PV (see Videos S1B to -D in the supplemental material), in contrast to the quiescence typical of tachyzoites (see Video S1A in the supplemental material). Developing bradyzoites can escape from the host cell and invade neighboring cells (Fig. 7A and C), but while tachyzoites typically lyse the host cell during their escape, bradyzoites frequently leave the host cell intact. In Fig. 7B, both parasites left the cell, leaving only a vestigial PV (continued observation by time-lapse microscopy confirmed long-term survival of this cell [data not shown]). Escaping bradyzoites appeared to be able to establish new bradyzoite cysts without reverting to tachyzoites. For example, the four parasites in Fig. 7A left the host cell at ~90 h postinduction. One parasite reinvaded the same host cell as a tachyzoite (left-most parasite), while three invaded the adjacent cell, establishing three independent vacuoles, two of which were stained with the bradyzoite-specific *Dolichos* lectin.

Figure 7C provides another example of bradyzoite motility (see the video displaying intermediate time points in the supplemental material), involving four zoites derived from a single PV. The first parasite escaped at ~23 h postinduction, simultaneously invading into an adjacent cell (parasite constriction was noted at the moving junction) (12). The second parasite followed 9 s later, establishing another PV in the same adjacent cell; the third parasite escaped into the supernatant medium 28 s later (37 s), and the fourth invaded into a different cell after a further 42 s (79 s). Approximately 1 min later (135 s), parasite 2 left its second host cell and invaded into yet another host cell. Note that the movement of these parasites frequently involved infection of adjacent cells without coming into contact with the external medium. Parasites continued to secrete the dense granule marker GRA8-YFP, and parasite 4 divided at ~71 h postinduction (shown in the fluorescent images).

The ability of parasites from a single vacuole to escape and reinvade multiple distinct PVs provides one mechanism by which several cysts might arise from a single infection (Fig. 7A and C). Surprisingly, bradyzoite vacuoles were also able to divide by fission, as shown in Fig. 7D, where the secreted GRA8-YFP reporter confirmed establishment of two distinct vacuoles. In some cases, one vacuole degenerated after several hours or days, while the other vacuole developed normally (data not shown). Figure 8 provides an extraordinary example of PV dynamics (see video in the supplemental material). At 24 h postinduction, four intracellular parasites were present in a single PV whose rounded nature and birefringence suggested that the differentiation process was under way. At ~34 h, nine zoites were visible, indicating asynchronous replication or en-

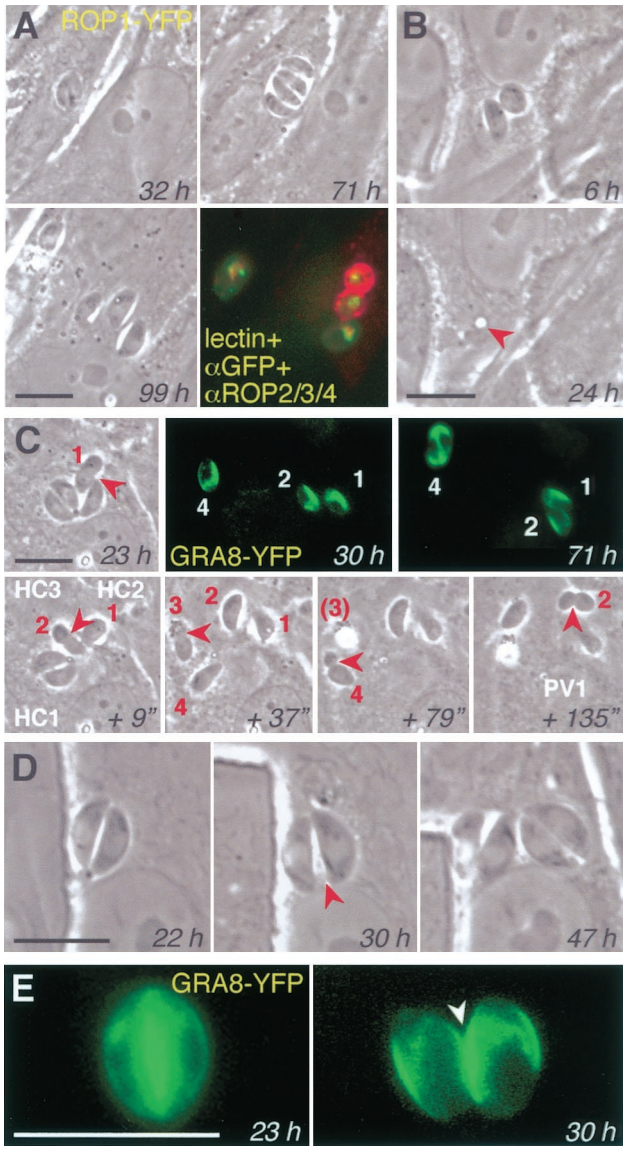

FIG. 7. Intracellular and intercellular motility of developing bradyzoites. (A) Differentiating ROP1-YFP transgenics divided only once from 32 to 71 h and then egressed from the originally infected host cell and invaded adjacent fibroblasts to establish four independent vacuoles. Fixation and staining with *D. biflorus* lectin (red) demonstrates variable levels of cyst wall development. (B) Egress of two parasites did not kill this host cell (which survived for several days) but left a residual PV "scar" (arrowhead). (C) Time-lapse series showing the escape of four GRA8-YFP transgenic parasites over the course of 135 s, all via moving junctions (arrowheads). Three parasites invaded directly into adjacent host cells (HC), with parasite 2 moving twice. GRA8-YFP expression (fluorescent panels) and parasite division indicated viability (many hours later). See Results for further description. (D and E) Fission of PVs during differentiation. Partition was preceded by motility of the zoites and proceeded while parasite division was in progress. Secretion of GRA8-YFP into the PV demonstrates that the two resulting vacuoles are not connected. Except for lectin staining and imunofluorescent assay, all panels show phase-contrast and fluorescence images of living parasites. Bars, 10 μm. See also the supplemental material for additional time-lapse images of bradyzoite motility in vitro and in vivo, including a video of the experiment shown in Fig. 7C.

dopolygeny. Seven of these parasites were seen in a new PV, while the other two remained behind. The two PVs remained connected for several minutes, as one parasite moved back and forth between the two. A secreted droplet of unknown composition was noted at the junction between the two PVs. At ~20 min, one parasite migrated from one side of the larger PV to the junction between the two vacuoles and, immediately upon contact, the two PVs separated. Although these two PVs appeared to be located in distinct cells, this seems unlikely, and the lack of a host cell marker precluded confirmation. Parasites within the smaller PV were highly motile for several hours while parasites within the larger vacuole were relatively quiescent, as this vacuole rounded up and became increasingly birefringent. Parasites in both PVs appeared to remain viable, dividing at ~48 h. Finally, the smaller PV moved, intact, to the proximity of the larger PV 20 min later. Parasites were fixed at this point and stained with *D. biflorus* lectin, demonstrating cyst wall material associated with both PVs. Collectively, Fig. 7 and 8 show that developing bradyzoites and bradyzoite cysts are highly dynamic.

In order to assess the frequency with which the unusual motility observed in bradyzoites occurs, a total of 510 vacuoles were followed for periods ranging from 4 to 9 days under bradyzoite differentiation conditions. Unusual motility was noted in a total of 5.5% of differentiating vacuoles, including 17 instances of intra- and/or intercellular motility giving rise to multiple vacuoles and 11 cases of vacuolar fission. Altering the conditions of cultivation (pH 6.2 to 8.2; [KCl] of 5 to 90 mM) had no significant effects on the level of parasite motility or vacuolar fission observed during differentiation induced by 0.03% CO_2 (data not shown). Although the low frequency of cyst formation prevented observation of these events during the early stages of bradyzoite differentiation in vivo, parasites were surprisingly motile within mature cysts isolated from the brains of chronically infected mice 8 weeks postinfection, in contrast to the highly quiescent nature of intracellular tachyzoites (see videos in the supplemental material).

DISCUSSION

In this study, we have described the early steps of *T. gondii* differentiation in vitro, which are summarized in Fig. 9. Exploiting of efficient in vitro differentiation methods, recombinant fusions of parasite proteins with fluorescent reporters, and time-lapse video microscopy of living cells has allowed us to follow the development of parasite bradyzoites. Although most of this work was conducted in vitro, rather than in the native parasitologic or host context (22), our studies recapitulate morphological characteristics known from static studies on fixed tissue cysts isolated from mouse brain, providing some confidence as to the validity of the in vitro differentiation system while providing a dynamic view indicating that differentiating parasites are remarkably motile.

Division in immature bradyzoites, quasi-mature cysts obtained in vitro, and mature tissue cysts. The exoenteric tachyzoite and mature bradyzoite (tissue cyst) stages of *T. gondii* divide primarily by endodyogeny, in which two daughter cells are assembled within the mother (15, 43), while asexual enteroepithelial precursors to gamete formation can divide by endodyogeny and schizogony, forming multiple daughter cells from

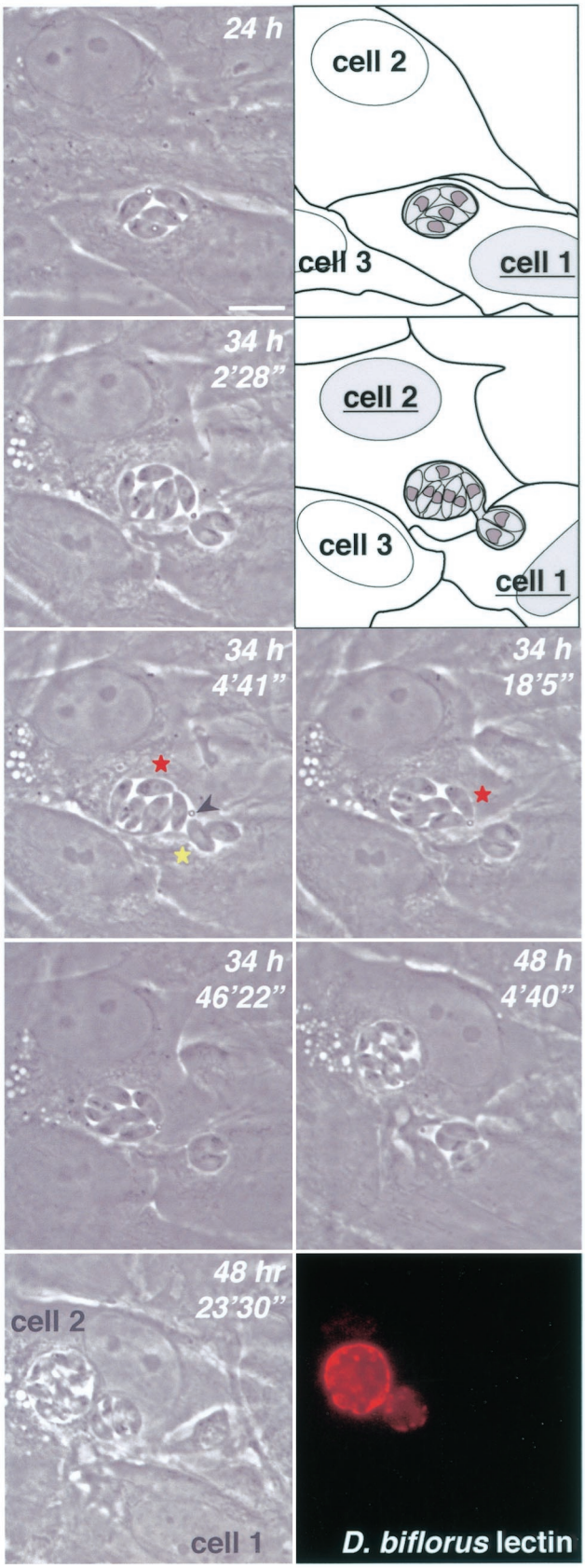

FIG. 8. Cyst fission, shown in a time-lapse series of living parasites demonstrating PV fission. Fixation and staining with *D. biflorus* lectin at the completion of the series shows cyst wall synthesis in both PVs. See Results for further description. Bars, 10 μm. Times reflect hours postinduction. See supplemental materials for a time-lapse video.

a single polyploid mother (14, 21). As expected from their slow growth rate, few divisions were observed in quasi-mature cysts cultivated in vitro, and these proceeded by endodyogeny (Fig. 1), consistent with electron microscopy studies on mature bradyzoites from mouse brain (15, 16, 18). In immature bradyzoites, endodyogeny was typically asynchronous (Fig. 2 and 3), and parasites were also observed to divide by cycles of schizogony or endopolygeny at a relatively high frequency.

What factor(s) controls division by endopolygeny and schizogony versus endodyogeny is unknown, but these processes are clearly part of a continuum of possibilities rather than the result of fundamentally different replicative mechanisms (25, 44). While the number of parasites per tissue cyst is highly variable (11), even within 10 days of differentiation in vitro, they may contain as many as hundreds of zoites (Fig. 1). Mechanisms that favor the rapid production of multiple daughters may be favored in the early stages of differentiation into a cyst that will then remain dormant for long periods of time. The DNA content of mature bradyzoites isolated from mouse brain suggests that these parasites are suspended in G_0 (M. White, personal communication), as observed in the transmitted stages of many protozoan parasites (34).

Morphological and metabolic modifications in immature bradyzoites. The earliest morphological changes in differentiating bradyzoites are associated with changes in secretion (Fig. 4). Although the precise function has yet not been defined for any dense granule protein, these proteins are suspected to play a role in maturation of the PV (7); they are therefore likely to be important for development of the cyst wall as well. Apparent reduction of the default secretory compartments (endoplasmic reticulum, dense granules) was noted within 2 days of induction, coincident with slowing of parasite replication. No alterations in rhoptry content and shape were detected in this study, but micronemes increased in number and became more widely distributed during differentiation, as has been noted in previous morphological studies.

An HSP60-YFP marker was used to label the mitochondrion, showing apparently normal morphology in both immature bradyzoites and quasi-mature cysts in vitro (Fig. 5). Fluorescence intensity declined during bradyzoite development in vitro, possibly reflecting reduced activity (although this has not been measured directly). Overall, function of the *T. gondii* mitochondrion remains poorly characterized (54), but changes in glycolysis appear early during differentiation (18) and energy metabolism is altered (8, 13, 32, 60). Previous studies have shown that electron transport chain inhibitors stimulate differentiation, suggesting reduced mitochondrial function in bradyzoites (2, 52). HSP60-positive posterior vesicular bodies (53) were not observed in the present study, perhaps reflecting differences between the in vitro system and mature bradyzoite cysts in animals.

Apicomplexan parasites harbor a second endosymbiotic organelle, the apicoplast, which is essential for tachyzoite survival although of unknown function (6, 19, 20, 24). Although the

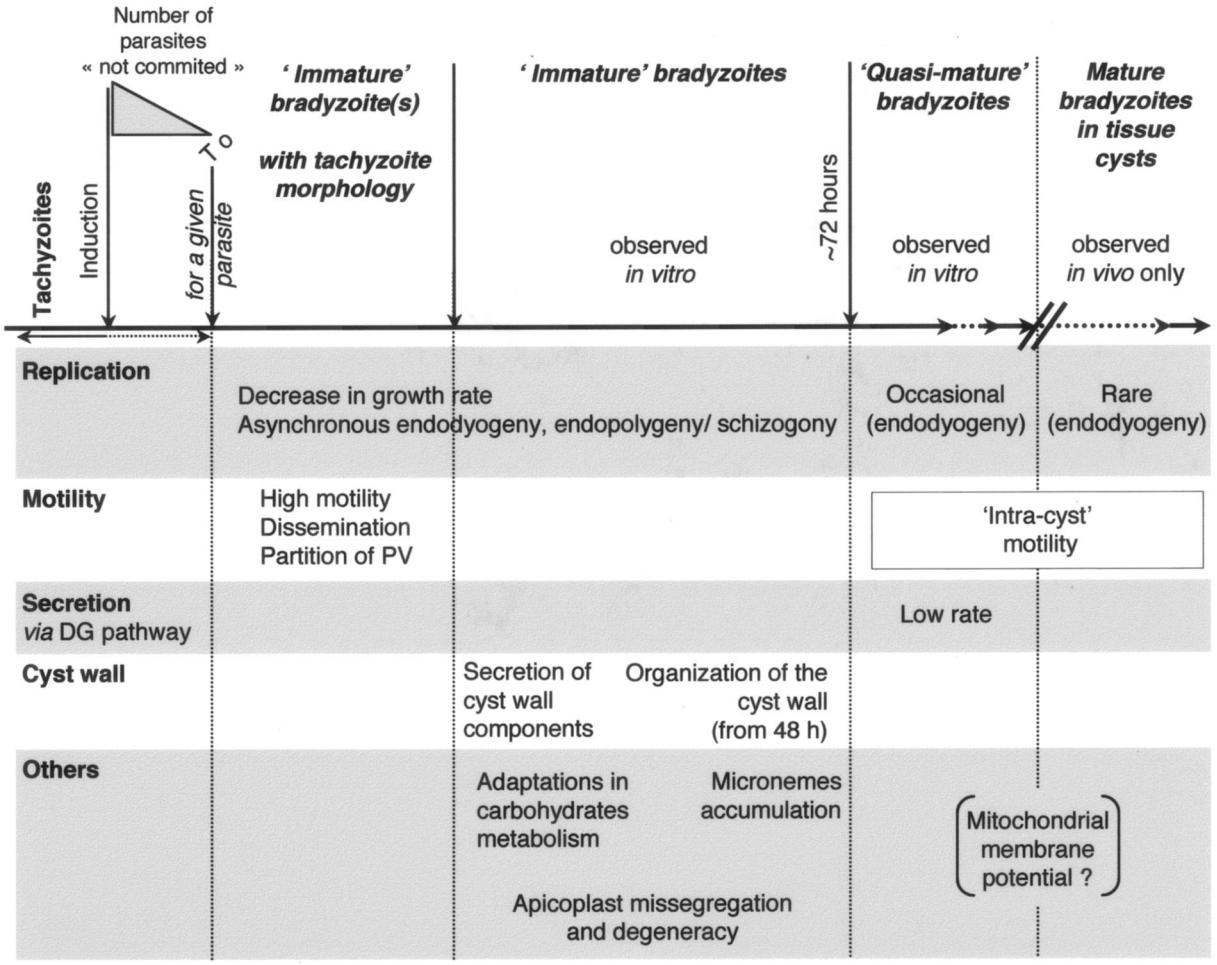

FIG. 9. Early stages of bradyzoite development in vitro.

apicoplast is efficiently maintained during tachyzoite replication (49), we were surprised to find that the organelle is lost in a significant number of parasites during bradyzoite differentiation (Fig. 6). The failure to detect either apicoplast DNA, a native apicoplast protein, or a transgenic apicoplast protein argues that the phenomenon is not an artifact of experimental detection, as confirmed by in vivo studies on mature brain cysts (Fig. 6G). Some evidence suggests that the apicoplast is required for initial establishment of a functional PV (19, 20, 24). It is highly unlikely that apicoplast-deficient parasites could regain this DNA-containing organelle, but the large number of parasites within a single tissue cyst is presumably sufficient to ensure propagation even if a few zoites have lost their apicoplast.

Highly dynamic nature of developing bradyzoites. At some point during bradyzoite differentiation (sometimes as long as 6 days postinduction), some of the quiescent intracellular parasites became unusually active, exhibiting high motility within the developing cyst, within the host cell, and even moving between host cells (Fig. 7 and 8; see also the videos in the supplemental material). Intravacuolar motility was also characteristic of mature encysted bradyzoites. In contrast, intracellular tachyzoites are noted for their quiescence (video in the supplemental material). The motility of extracellular tachyzoites is dramatically affected by ionic conditions, facilitating egress from dying host cells (35, 38, 40). Although we did not observe any variation in bradyzoite motility when parasites were induced to differentiate at low or high pH, or at high potassium concentrations, bradyzoite motility may be associated with as-yet-undefined conditions, such as other ionic changes in either the parasite or host cell during the induction of differentiation.

Motile bradyzoites were capable of leaving the host cell without killing it (Fig. 7) and invading a new host cell—a phenomenon reminiscent of the transepithelial migration by tachyzoites during infection (1) and the ability of sporozoites to pass completely through multiple host cells (37, 47). We have not studied the behavior of individual bradyzoites in great detail, but their motility appears superficially similar to that of other parasite zoites (1, 36). Egress of multiple parasites from a single developing cyst was usually asynchronous but always involved a moving junction similar to that observed during tachyzoite invasion (cf. Fig. 7C and the video in the supplemental material). This process yields multiple vacuoles from a single infection, and bradyzoite-specific markers began to appear immediately upon establishment of these new vacuoles. Immature bradyzoites were also able to establish multiple vacuoles by partitioning individual cysts (Fig. 7D and 8).

The mechanism underlying these processes is unclear, but they occur sufficiently often to help in explaining the observed increase in tissue cyst burden in the brains of chronically infected animals, despite the low frequency of cyst rupture (17). *T. gondii* parasites are capable of forming tissue cysts in multiple cell types (30), but different culture conditions dramatically affect the frequency of encystment in vitro. In vivo, cysts occur most commonly in neuronal cells within the brain (16), and host cells outside the mitotic cell cycle may represent a preferred environment for *T. gondii* differentiation. The unexpected motility of differentiating bradyzoites observed by time-lapse microscopy provides a possible mechanism for parasites to move to an appropriate host cell once the commitment to differentiate has been made. It is even possible that cell-to-cell spread is required for differentiation, as appears to be the case for conversion of sporozoites to tachyzoites (51). Overall, it appears that immature bradyzoites are remarkably dynamic. They are highly motile within and between host cells, partition their PVs, rapidly synthesize cyst wall components, and reorganize organelles—all in the first few days of the differentiation process.

ACKNOWLEDGMENTS

We thank John Murray and Ke Hu for helpful discussions and Michael J. Crawford for critical reading of the manuscript. The laboratory of Christopher Hunter provided advice and assistance with animal studies, and we also appreciate the generosity of the many investigators who provided parasites, plasmids, and antibodies, as noted in Materials and Methods.

This research was supported by grants from the National Institutes of Health and a fellowship from Fondation pour la Recherche Médicale.

REFERENCES

1. **Barragan, A., and L. D. Sibley.** 2002. Transepithelial migration of *Toxoplasma gondii* is linked to parasite motility and virulence. J. Exp. Med. **195:**1625–1633.
2. **Bohne, W., J. Heesemann, and U. Gross.** 1994. Reduced replication of *Toxoplasma gondii* is necessary for induction of bradyzoite-specific antigens: a possible role for nitric oxide in triggering stage conversion. Infect. Immun. **5:**1761–1767.
3. **Bohne, W., U. Gross, D. J. Ferguson, and J. Heesemann.** 1995. Cloning and characterization of a bradyzoite-specifically expressed gene (hsp30/bag1) of *Toxoplasma gondii*, related to genes encoding small heat-shock proteins of plants. Mol. Microbiol. **16:**1221–1230.
4. **Bohne, W., and D. S. Roos.** 1997. Stage-specific expression of a selectable marker in *Toxoplasma gondii* permits selective inhibition of either tachyzoites or bradyzoites. Mol. Biochem. Parasitol. **88:**115–126.
5. **Boothroyd, J. C., M. Black, S. Bonnefoy, A. Hehl, L. J. Knoll, I. D. Manger, E. Ortega-Barria, and S. Tomavo.** 1997. Genetic and biochemical analysis of development in *Toxoplasma gondii.* Phil. Trans. R. Soc. London B **352:**1347–1354.
6. **Camps, M., G. Arrizabalaga, and J. Boothroyd.** 2002. An rRNA mutation identifies the apicoplast as the target for clindamycin in *Toxoplasma gondii.* Mol. Microbiol. **43:**1309–1318.
7. **Cesbron-Delauw, M. F., L. Lecordier, and C. Mercier.** 1996. Role of secretory dense granule organelles in the pathogenesis of toxoplasmosis. Curr. Top. Microbiol. Immunol. **219:**59–65.
8. **Denton, H., C. W. Roberts, J. Alexander, K. W. Thong, and G. H. Coombs.** 1996. Enzymes of energy metabolism in the bradyzoites and tachyzoites of *Toxoplasma gondii.* FEMS Microbiol. Lett. **15:**103–108.
9. **Donald, R. G., and D. S. Roos.** 1993. Stable molecular transformation of *Toxoplasma gondii*: a selectable dihydrofolate reductase-thymidylate synthase marker based on drug-resistance mutations in malaria. Proc. Natl. Acad. Sci. USA **90:**11703–11707.
10. **Dubey, J. P., and J. K. Frenkel.** 1976. Feline toxoplasmosis from acutely infected mice and the development of *Toxoplasma* cysts. J. Protozool. **23:**537–546.
11. **Dubey, J. P., D. S. Lindsay, and C. A. Speer.** 1998. Structures of *Toxoplasma gondii* tachyzoites, bradyzoites, and sporozoites and biology and development of tissue cysts. Clin. Microbiol. Rev. **11:**267–299.
12. **Dubremetz, J. F., N. Garcia-Réguet, V. Conseil, and M. N. Fourmaux.** 1998. Apical organelles and host-cell invasion by Apicomplexa. Int. J. Parasitol. **28:**1007–1013.
13. **Dzierszinski, F., M. Mortuaire, N. Dendouga, O. Popescu, and S. Tomavo.** 2001. Differential expression of two plant-like enolases with distinct enzymatic and antigenic properties during stage conversion of the protozoan parasite *Toxoplasma gondii.* J. Mol. Biol. **309:**1017–1027.
14. **Ferguson, D. J., W. M. Hutchison, J. F. Dunachie, and J. C. Siim.** 1974. Ultrastructural study of early stages of asexual multiplication and microgametogony of *Toxoplasma gondii* in the small intestine of the cat. Acta Pathol. Microbiol. Scand. B **82:**167–181.
15. **Ferguson, D. J., and W. M. Hutchison.** 1987. An ultrastructural study of the early development and tissue cyst formation of *Toxoplasma gondii* in the brains of mice. Parasitol. Res. **73:**483–491.
16. **Ferguson, D. J., and W. M. Hutchison.** 1987. The host-parasite relationship of *Toxoplasma gondii* in the brains of chronically infected mice. Virchows Arch. **411:**39–43.
17. **Ferguson, D. J., W. M. Hutchison, and E. Pettersen.** 1989. Tissue cyst rupture in mice chronically infected with *Toxoplasma gondii.* An immunocytochemical and ultrastructural study. Parasitol. Res. **75:**599–603.
18. **Ferguson, D. J., S. Parmley, and S. Tomavo.** 2002. Evidence for nuclear localisation of two stage-specific isoenzymes of enolase in *Toxoplasma gondii* correlates with active parasite replication. Int. J. Parasitol. **32:**1399–1410.
19. **Fichera, M. E., M. K. Bhopale, and D. S. Roos.** 1995. In vitro assays elucidate peculiar kinetics of clindamycin action against *Toxoplasma gondii.* Antimicrob. Agents Chemother. **39:**1530–1537.
20. **Fichera, M. E., and D. S. Roos.** 1997. A plastid organelle as a drug target in apicomplexan parasites. Nature **390:**407–409.
21. **Frenkel, J. K.** 1973. Toxoplasmosis: parasite life cycle, pathology and immunology, p. 343–410. *In* D. M. Hammond and P. L. Long (ed.), The Coccidia. University Park Press, Baltimore, Md.
22. **Frenkel, J. K.** 1996. The stage-conversion time of *Toxoplasma gondii*: interpretation of chemical-biologic data out of parasitologic or host context. Parasitol. Res. **82:**656–658.
23. **Hager, K. M., B. Striepen, L. G. Tilney, and D. S. Roos.** 1999. The nuclear envelope serves as an intermediary between the ER and Golgi complex in the intracellular parasite *Toxoplasma gondii.* J. Cell Sci. **112:**2631–2638.
24. **He, C. Y., M. K. Shaw, C. H. Pletcher, B. Striepen, L. G. Tilney, and D. S. Roos.** 2001. A plastid segregation defect in the protozoan parasite *Toxoplasma gondii.* EMBO J. **20:**30–39.
25. **Hu, K., T. Mann, B. Striepen, C. J. Beckers, D. S. Roos, and J. M. Murray.** 2002. Daughter cell assembly in the protozoan parasite *Toxoplasma gondii.* Mol. Biol. Cell **13:**593–606.
26. **Jomaa, H., J. Wiesner, S. Sanderbrand, B. Altincicek, C. Weidemeyer, M. Hintz, I. Turbachova, M. Eberl, J. Zeidler, H. K. Lichtenthaler, D. Soldati, and E. Beck.** 1999. Inhibitors of the nonmevalonate pathway of isoprenoid biosynthesis as antimalarial drugs. Science **285:**1573–1576.
27. **Kim, K., D. Soldati, and J. C. Boothroyd.** 1993. Gene replacement in *Toxoplasma gondii* with chloramphenicol acetyltransferase as selectable marker. Science **262:**911–914.
28. **Köhler, S., C. F. Delwiche, P. W. Denny, L. G. Tilney, P. Webster, R. J. Wilson, J. D. Palmer, and D. S. Roos.** 1997. A plastid of probable green algal origin in apicomplexan parasites. Science **275:**1485–1489.
29. **Levine, N. D.** 1988. Progress in taxonomy of the apicomplexan protozoa. J. Protozool. **35:**518–520.
30. **Lindsay, D. S., J. P. Dubey, B. L. Blagburn, and M. Toivio-Kinnucan.** 1991. Examination of tissue cyst formation by *Toxoplasma gondii* in cell cultures using bradyzoites, tachyzoites, and sporozoites. J. Parasitol. **77:**126–132.
31. **Luft, B. J., and J. S. Remington.** 1992. Toxoplasmic encephalitis in AIDS. Clin. Infect. Dis. **15:**211–222.
32. **Manger, I. D., A. Hehl, S. Parmley, L. D. Sibley, M. Marra, L. Hillier, R. Waterston, and J. C. Boothroyd.** 1998. Expressed sequence tag analysis of the bradyzoite stage of *Toxoplasma gondii*: identification of developmentally regulated genes. Infect. Immun. **66:**1632–1637.
33. **Matrajt, M., M. Nishi, M. J. Fraunholz, O. Peter, and D. S. Roos.** 2002. Amino-terminal control of transgenic protein expression levels in *Toxoplasma gondii.* Mol. Biochem. Parasitol. **120:**285–289.
34. **Milon, G., and P. H. David.** 1999. Transmission stages of *Plasmodium*: does the parasite use the one same signal, provided both by the host and the vector, for gametocytogenesis and sporozoite maturation? Parassitologia **41:**159–162.
35. **Mondragon, R., and E. Frixione.** 1996. Ca^{2+}-dependence of conoid extrusion in *Toxoplasma gondii* tachyzoites. J. Eukaryot. Microbiol. **43:**120–127.
36. **Morisaki, J. H., J. E. Heuser, and L. D. Sibley.** 1995. Invasion of *Toxoplasma gondii* occurs by active penetration of the host cell. J. Cell Sci. **108:**2457–2464.
37. **Mota, M. M., J. C. Hafalla, and A. Rodriguez.** 2003. Corrigendum: migration through host cells activates *Plasmodium* sporozoites for infection. Nat. Med. **9:**146.
38. **Moudy, R., T. J. Manning, and C. J. Beckers.** 2001. The loss of cytoplasmic potassium upon host cell breakdown triggers egress of *Toxoplasma gondii.* J. Biol. Chem. **276:**41492–41501.

39. **Nagel, S. D., and J. C. Boothroyd.** 1988. The alpha- and beta-tubulins of *Toxoplasma gondii* are encoded by single copy genes containing multiple introns. Mol. Biochem. Parasitol. **29:**261–273.
40. **Pingret, L., J. M. Millot, S. Sharonov, A. Bonhomme, M. Manfait, and J. M. Pinon.** 1996. Relationship between intracellular free calcium concentrations and the intracellular development of *Toxoplasma gondii.* J. Histochem. Cytochem. **44:**1123–1129.
41. **Roos, D. S.** 1993. Primary structure of the dihydrofolate reductase-thymidylate synthase gene from *Toxoplasma gondii.* J. Biol. Chem. **268:**6269–6280.
42. **Roos, D. S., R. G. Donald, N. S. Morrissette, and A. L. Moulton.** 1994. Molecular tools for genetic dissection of the protozoan parasite *Toxoplasma gondii*. Methods Cell Biol. **45:**27–63.
43. **Roos, D. S., M. J. Crawford, R. G. K. Donald, J. C. Kissinger, L. J. Klimczak, and B. Striepen.** 1999. Origins, targeting, and function of the apicomplexan plastid. Curr. Opin. Microbiol. **2:**426–432.
44. **Sheffield, H. G., and M. L. Melton.** 1968. The fine structure and reproduction of *Toxoplasma gondii.* J. Parasitol. **54:**209–226.
45. **Soête, M., B. Fortier, D. Camus, and J. F. Dubremetz.** 1993. *Toxoplasma gondii*: kinetics of bradyzoite-tachyzoite interconversion *in vitro.* Exp. Parasitol. **76:**259–264.
46. **Soête, M., D. Camus, and J. F. Dubremetz.** 1994. Experimental induction of bradyzoite-specific antigen expression and cyst formation by the RH strain of *Toxoplasma gondii in vitro.* Exp. Parasitol. **78:**361–370.
47. **Speer, C. A., J. P. Dubey, J. A. Blixt, and K. Prokop.** 1997. Time lapse video microscopy and ultrastructure of penetrating sporozoites, types 1 and 2 parasitophorous vacuoles, and the transformation of sporozoites to tachyzoites of the VEG strain of *Toxoplasma gondii.* J. Parasitol. **83:**565–574.
48. **Striepen, B., C. Y. He, M. Matrajt, D. Soldati, and D. S. Roos.** 1998. Expression, selection, and organellar targeting of the green fluorescent protein in *Toxoplasma gondii.* Mol. Biochem. Parasitol. **92:**325–338.
49. **Striepen, B., M. J. Crawford, M. K. Shaw, L. G. Tilney, F. Seeber, and D. S. Roos.** 2000. The plastid of *Toxoplasma gondii* is divided by association with the centrosomes. J. Cell Biol. **151:**1423–1434.
50. **Striepen, B., D. Soldati, N. Garcia-Réguet, J. F. Dubremetz, and D. S. Roos.** 2001. Targeting of soluble proteins to the rhoptries and micronemes in *Toxoplasma gondii.* Mol. Biochem. Parasitol. **113:**45–53.
51. **Tilley, M., M. E. Fichera, M. E. Jerome, D. S. Roos, and M. W. White.** 1997. *Toxoplasma gondii* sporozoites form a transient parasitophorous vacuole that is impermeable and contains only a subset of dense-granule proteins. Infect. Immun. **65:**4598–4605.
52. **Tomavo, S., and J. C. Boothroyd.** 1995. Interconnection between organellar functions, development and drug resistance in the protozoan parasite *Toxoplasma gondii.* Int. J. Parasitol. **25:**1293–1299.
53. **Toursel, C., F. Dzierszinski, A. Bernigaud, M. Mortuaire, and S. Tomavo.** 2000. Molecular cloning, organellar targeting and developmental expression of mitochondrial chaperone HSP60 in *Toxoplasma gondii.* Mol. Biochem. Parasitol. **111:**319–332.
54. **Vercesi, A. E., C. O. Rodrigues, S. A. Uyemura, L. Zhong, and S. N. Moreno.** 1998. Respiration and oxidative phosphorylation in the apicomplexan parasite *Toxoplasma gondii.* J. Biol. Chem. **273:**31040–31047.
55. **Vollmer, M., N. Thomsen, S. Wiek, and F. Seeber.** 2001. Apicomplexan parasites possess distinct nuclear-encoded, but apicoplast-localized, plant-type ferredoxin-NADP$^+$ reductase and ferredoxin. J. Biol. Chem. **276:**5483–5490.
56. **Waller, R. F., P. J. Keeling, R. G. Donald, B. Striepen, E. Handman, N. Lang-Unnasch, A. F. Cowman, G. S. Besra, D. S. Roos, and G. I. McFadden.** 1998. Nuclear-encoded proteins target to the plastid in *Toxoplasma gondii* and *Plasmodium falciparum.* Proc. Natl. Acad. Sci. USA **95:**12352–12357.
57. **Weiss, L. M., D. Laplace, P. M. Takvorian, H. B. Tanowitz, A. Cali, and M. Wittner.** 1995. A cell culture system for study of the development of *Toxoplasma gondii* bradyzoites. J. Eukaryot. Microbiol. **42:**150–157.
58. **Weiss, L. M., and K. Kim.** 2000. The development and biology of bradyzoites of *Toxoplasma gondii.* Front. Biosci. **5:**D391–D405.
59. **Yahiaoui, B., F. Dzierszinski, A. Bernigaud, C. Slomianny, D. Camus, and S. Tomavo.** 1999. Isolation and characterization of a subtractive library enriched for developmentally regulated transcripts expressed during encystation of *Toxoplasma gondii.* Mol. Biochem. Parasitol. **99:**223–235.
60. **Yang, S., and S. F. Parmley.** 1997. *Toxoplasma gondii* expresses two distinct lactate dehydrogenase homologous genes during its life cycle in intermediate hosts. Gene **184:**1–12.
61. **Zhang, Y. W., S. K. Halonen, Y. F. Ma, M. Wittner, and L. M. Weiss.** 2001. Initial characterization of CST1, a *Toxoplasma gondii* cyst wall glycoprotein. Infect. Immun. **69:**501–507.